Supporting Information

Characterizing the Metal-SAM Interface in Tunneling Junctions

Carleen M. Bowers,[1,‡] Kung-Ching Liao,[1,‡] Tomasz Żaba,[2] Dmitrij Rappoport,[1] Mostafa Baghbanzadeh,[1] Benjamin Breiten,[1] Anna Krzykawska,[2] Piotr Cyganik,[2] and George M. Whitesides[1,3*]

[1]Department of Chemistry and Chemical Biology, Harvard University,
12 Oxford Street, Cambridge, Massachusetts 02138 United States

[1]Smoluchowksi Institue of Physics, Jagiellonian University,
Reymonta 4, 30-059 Krakow, Poland

[3]Kavli Institute for Bionano Science & Technology, Harvard University,
29 Oxford Street, Massachusetts 02138 United States

*Corresponding author, email: gwhitesides@gmwgroup.harvard.edu

[‡] These authors contributed equally to this work

Experimental Details

Materials. Precursors to all monolayers were commercially available (≥ 98%, Sigma-Aldrich). All organic solvents were analytical grade (99%, Sigma-Aldrich) and were used as supplied unless otherwise specified. All compounds were maintained under a N_2 atmosphere at < 4°C to avoid decomposition. To ensure that the compounds were free of contaminants, all stored compounds were checked by ^1H NMR prior to use. Impurities were carefully removed by silica gel column chromatography (100% hexane).

SAMs of *n*-alkanecarboxylates on silver electrodes. In studies that relate the organic structure of molecules making up a monolayer in a junction to rates of charge transport across that junction, SAMs based on *n*-alkanethiolates have been studied extensively because they are commercially available, well-characterized—both in terms of their physical properties and their electronic properties, especially as an insulating component in electrical junctions[1-6]—and are highly-structured.[7] We recently characterized SAMs of *n*-alkanecarboxylates (*n*-alkanoates) on silver[8] as a potential substitute to *n*-alkanethiolates for measuring rates of charge transport. Alkanoic acids present an attractive alternative to thiolates as they eliminate their oxidative instabilities, and are also available commercially in a wide range of structures. SAMs of *n*-alkanoates form well-organized and densely packed monolayers on metal oxide substrates (i.e., Ag, Cu, Al); long chain *n*-alkanoates on Ag, in particular, result in crystalline packing in an all-*trans* conformation with a tilt angle between 15º and 25º (from the surface normal).[9] The carboxylate headgroup coordinates with Ag (and its native oxide) through ionic interactions (bidentate ionic binding coordination); this ionic interface disassociates upon exposure to sources of protons (e.g., HCl or H_2S vapor).[10, 11]

Preparation of *n*-Alkyne SAMs on template-stripped gold (Au^{TS}) bottom electrodes. We formed SAMs on four hundred-nanometer thick template-stripped gold (Au^{TS}).[12] SAMs formed on template stripped metal surfaces have less defects than SAMs on as-deposited surfaces, and result in junction measurements with higher yields and with smaller dispersions in J(V) than as-deposited bottom electrodes.[13, 14] Au^{TS} substrates were submerged in a 6-mM solution of alkyne in anhydrous hexadecane for 48 hours at room temperature and under a nitrogen atmosphere. (The temperature was kept at room temperature (ca. 23°C) due to the instability of the optical adhesive at higher temperatures). The alkynes on gold are susceptible to oxidation in the presence of oxygen; therefore additional care was exercised to minimize exposure of the substrate and solution to oxygen. We rinsed the SAM-bound substrates with hexadecane, followed by ethanol, and dried them under a gentle stream of nitrogen. We characterized the SAMs with X-ray photoelectron spectroscopy (XPS; Thermo Scientific K-Alpha photoelectron spectrometer with Monochromatic Al K-α X-ray radiation (1.49 kV at base pressure ~10^{-9} Torr)) and water contact angle analysis to monitor the presence of oxygen in the SAM (Figure S1 and Table S1).

Preparation of *n*-alkyne SAMs on Au evaporated on mica (Au^{Mica}) bottom electrodes. SAMs of decyne and tetradecyne were formed on flame-annealed gold that was evaporated on mica (~150 nm of Au on mica) according to a procedure described in a separate report.[15] The Au^{mica} substrates were submerged in 1mM alkyne in ethanol for 15 hours at 60°C. To avoid oxidation of the acetylene group during formation of the SAM, the SAMs were formed under N_2 using only freshly evaporated Au(111) substrates. Immediately before electrical measurements, the samples were removed from the solution, rinsed with ethanol, and dried under N_2.

Preparation of *n*-alkanethiolate SAMs on template-stripped gold (Au[TS]) bottom electrodes. SAMs of *n*-alkanethiolates served as internal standards for this work, and ensured that the apparatus and the operators were reproducing previous values of current densities.[16] We followed previously published protocols for the formation of SAMs on Au[TS].[16-18] Briefly, Au[TS] substrates were submerged in a 3mM ethanolic solution of thiolate for 16-18 hours at room temperature and under a nitrogen atmosphere. We rinsed the SAM-bound substrates with ethanol, and dried them under a gentle stream of nitrogen.

DFT Computational Details. The frontier orbital energies were calculated with density functional theory (DFT) using the Becke hybrid functional B3-LYP[19] and resolution-of-the-identity approximation for the Coulomb energy (RI-J);[20] def2-SVP Gaussian basis sets were used along with corresponding auxiliary basis sets[21] and small-core relativistic effective core potentials (ECPs) for Ag.[22] All calculations were carried out within the Turbomole suite of programs (V6.4, 2012).

Electrical measurements using EGaIn. EGaIn (eutectic Ga-In; 74.5% Ga, 25.5% In)—a liquid metal with a self-passivating oxide layer of Ga_2O_3—serves as a convenient and non-damaging top-contact for measuring currents across self-assembled monolayers (SAMs) in junction devices having the structure Met[TS]/SAM//Ga_2O_3/EGaIn.[23, 24] The mechanical properties of the electrically conducting Ga_2O_3 film that forms on the surface facilitates the formation of sharp conical tips (enabling a small geometrical footprint of ~25 μm in diameter, or ~490 μm^2 in geometrical contact area estimated by microscopy).[16] We selected EGaIn conical tips that were free of visible surface asperities.[25] We measured charge-transport across the SAMs at ±0.5 V by sweeping in both directions starting at 0 V (i.e., one sweep 0 V → +0.5 V → 0 V → 0.5 V → 0 V, in steps of 0.05 V). For each compound, we collected ~400 – 800 *J–V* traces from three to

four substrates; the yield of working junctions was $\geq$ 86% (Table S2). The approximately log-normal distribution of data for J(V) justified a Gaussian fitting for each histogram; this fitting provided mean values of $\log|J|$ ($\log|J_{mean}|$) and standard deviations (σ_{log}) (Figure S2). Values of σ_{log} varied from 0.3 to 0.6—values similar to those obtained for measurements across SAMs of n-alkanethiolates.[15] Electrical measurements across SAMs having oxygen-containing contaminants (most likely due to the decomposition of the acetylene molecules following exposure to oxygen and gold) are shown in Figure S3. These oxygen-containing SAMs result in slightly lower values (by a factor of ~5) of current density than oxygen-free SAMs.

Characteristics of a tunneling barrier. In measurements of charge transport across an electrode–SAM–electrode junction, charges encounter a tunneling barrier whose shape is determined by the electrical characteristics of three principle components: the SAM, the electrodes, and the interfaces between the SAM and the electrodes. The Simmons equation[26] (eq.1) reliably predicts that the rate of charge transport decays exponentially with increasing width of the tunneling barrier (and the parameter d is often approximated as the distance between the two electrodes). In this paper, we estimate d by the calculated length of the molecules making up the SAM, or by the thickness of the SAM (in Å or number of CH_2 units). The injection current, J_0(V), is the value of J(V) expected for a hypothetical junction with $d = 0$, but with interfaces characteristic of a SAM-containing junction. The attenuation of current is described by the value of β—a value that is determined by the shape (e.g., height; for a rectangular barrier) of the tunneling barrier—and is related to the electronic structure of the molecules in ways that are still not completely defined.[27]

The energetic topography of the tunneling barrier, and the tunneling currents have emerged as surprisingly simple. The methylene chain of alkyl-based SAMs seems to be adequately

approximated by a rectangular tunneling barrier of the type described by the simplified Simmons equation (Eq. 1);[26] a number of substitutions for the terminal group T (including a wide but not completely inclusive range of simple aromatic and aliphatic groups,[28] and charged[25] and neutral[29] polar groups) are indistinguishable in their influence on tunneling currents, so long as the SAMs have the same thickness. Groups, M, in the center of the chain (amides (–CONH– and –NHCO–) and urea (–NHCONH–))[6] are also indistinguishable from oligomethylene chains (–$(CH_2)_n$–) of the same thickness. Certain groups whose molecular orbitals (MOs) align with the Fermi energy level of the metal—for example, ferrocene,[30-33] bipyridyl,[34] and anthraquinone,[35] *can* influence the tunneling current density (J(V), Acm^{-2}).

Influence of oxygen contaminants in SAMs of alkynes on tunneling currents. The nature of the interfacial bond *is* important for the organization of the alkyl molecular layer, whose order may influence charge transport. In the case of SAMs of alkynes, measurements of current density are sensitive to adventitious oxidation; oxidation of the SAM detectable by XPS resulted in a decrease in current density by a factor of ~5. Junctions composed of oxygen-free (< 5% oxygen) SAMs of alkynes and of alkanethiolates on gold gave indistinguishable values of J_0 (3.9 ± 0.1 and 4.2 ± 0.2 A/cm^2). The measured value of β for *n*-alkynes (0.67± 0.02 Å^{-1}), however, appears slightly lower than that for *n*-alkanethiolates (0.76 ± 0.02 Å^{-1}); we tentatively attribute this small deviation to differences in the structure of SAMs composed of the short alkyl groups.

Interpretation of the tunneling decay constant, β. The small apparent difference in the values for β between *n*-alkynes and *n*-alkanethiolates might be due to a small but real difference in the rates of tunneling across these systems (when appropriately compared), to differences in the method used in estimation of the width of the tunneling barrier, or to small differences in the experimental systems. Figure 2, in the main text, considers the distance of the tunneling barrier,

in Å, to be from the anchoring atom to the final hydrogen atom; this estimation does not consider possible differences in the structure of the SAMs that might not be apparent from the available spectroscopic methods (i.e. variations in tilt, twist and torsion angles between SAMs of *n*-alkynes and SAMs of *n*-alkanethiolates[15]). Therefore, we also consider the total width of the tunneling barrier in terms of the film-thickness of the SAM for *n*-alkynes and *n*-alkanethiolates on gold; a plot of *J*(V) *versus* effective thickness[15] is included in the supporting information (Figure S6). This analysis also revealed indistinguishable attenuation factors for of *n*-alkynes and *n*-alkanethiolates ($\beta = 0.90 \pm 0.07$ Å^{-1} for *n*-alkynes; $\beta = 0.97 \pm 0.05$ Å^{-1} for *n*-alkanethiolates).

Table S1. Summary of static water-wetting contact angles (θ_s) for *n*-alkynes on Au^{TS} and advancing (θ_a) and receding water contact angle (θ_r) for *n*-alkanethiolates on Au. The advancing (θ_a) and receding contact angle (θ_r) data for hexadecanethiol were taken from reference 14.

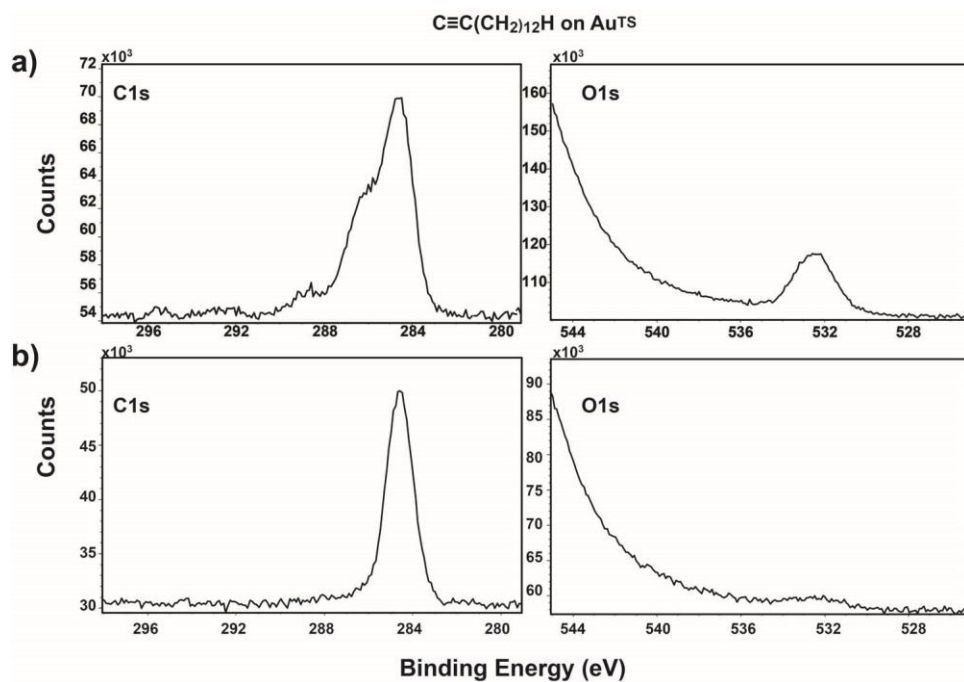| Alkynes on Au^{TS}	mean contact angle (θ_s) and standard	Alkanethiolate on Au	contact angle (θ_a, θ_r)[9]
C≡C(CH$_2$)$_4$H	103± 2	S(CH$_2$)$_{16}$H	~115, ~ 105
C≡C(CH$_2$)$_6$H	103 ± 1		
C≡C(CH$_2$)$_8$H	103 ± 1		
C≡C(CH$_2$)$_{10}$H	104 ± 1		
C≡C(CH$_2$)$_{12}$H	108 ± 1		

Figure S1. XPS spectra of O1s and C1s regions from a) oxidized SAMs of tetradecyne on Au[TS] and b) neutral SAMs of tetradecyne on Au.[TS]

Table S2. Summary of the data collected for measurements of $J(V)$ across $Au^{TS}/C\equiv C(CH_2)_nH//Ga_2O_3/EGaIn$ and $Au^{TS}/S(CH_2)_nH//Ga_2O_3/EGaIn$ at +0.5 V.

			n-Alkynes		*n*-Alkanethiolates[4]	
$C\equiv CC_n$	N[1]	Yield[2] (%)	Traces[3]	Log $|J|_{mean} \pm \sigma_{log}$ (Acm^{-2})	SC_n	Log $|J|_{mean} \pm \sigma_{log}$ (Acm^{-2})
$C\equiv CC_4$	3	88	503	1.8 ± 0.5		
$C\equiv CC_6$	3	87	421	1.1 ± 0.4	SC_6	1.2 ± 0.4
$C\equiv CC_8$	3	87	458	0.5 ± 0.3	SC_8	0.5 ± 0.5
$C\equiv CC_{10}$	3	96	626	-0.4 ± 0.4	SC_{10}	-0.3 ± 0.5
$C\equiv CC_{12}$	4	97	800	-1.1 ± 0.6	SC_{12}	-1.3 ± 0.6
					SC_{14}	-2.1 ± 0.5

[1] N is the number of independent samples that were measured
[2] % Yield was calculated from the number of working (i.e. non-shorting) junctions divided by the total number of junctions that were measured
[3] Trace is a sweep that generates two data points from the forward and reverse bias
[4] The data for alkanethiolates were collected for this study and not taken from a literature reference

Table S3. Calculated energies for the HOMO of *n*-alkanethiolates and *n*-alkynes on gold clusters using density functional theory (DFT).[19-23] The HOMO, S and HOMO, C indicate the orbital centered on the anchoring atom. The MO, C-C indicates the orbital energies from the C-C bonds along the alkyl chain.

SAM on Au	HOMO, S (eV)	MO, C-C (eV)	SAM on Au	HOMO, C (eV)	MO, C-C (eV)
SC_2H_5	-5.62	-	$C{\equiv}CC_4H_9$	-6.15	-8.89
SC_4H_9	-5.61	-8.39	$C{\equiv}CC_6H_{13}$	-6.15	-8.61
SC_6H_{13}	-5.61	-8.37	$C{\equiv}CC_8H_{17}$	-6.15	-8.38
SC_8H_{17}	-5.61	-8.11	$C{\equiv}CC_{10}H_{21}$	-6.15	-8.16
$SC_{10}H_{21}$	-5.61	-8.09	$C{\equiv}CC_{12}H_{25}$	-6.15	-8.05
$SC_{12}H_{25}$	-5.60	-8.08	$C{\equiv}CC_{14}H_{29}$	-6.15	-8.00
$SC_{14}H_{29}$	-5.61	-7.88			
$SC_{16}H_{33}$	-5.61	-7.88			
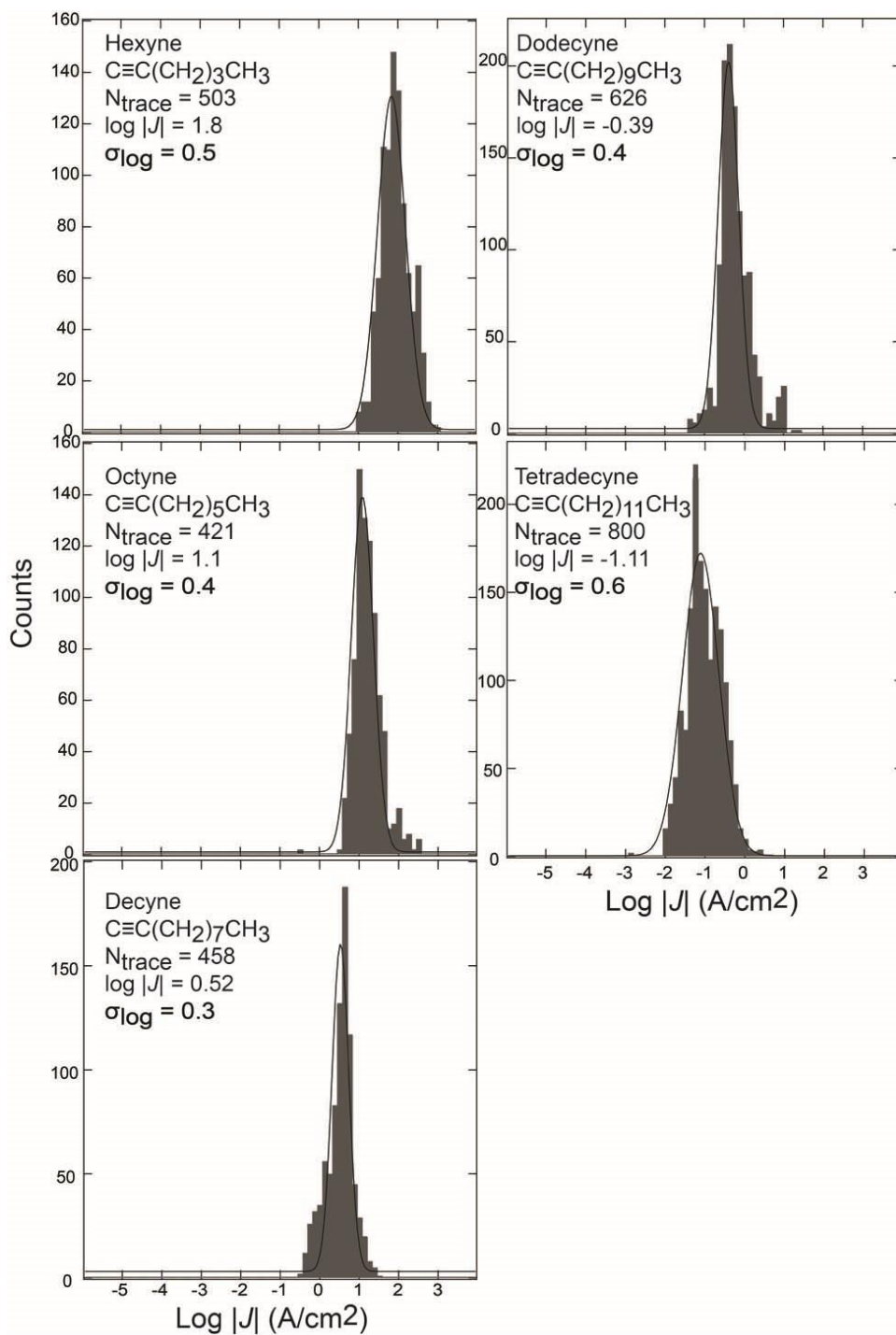
Figure S2. Histograms of log|J| at +0.5 V for acetylene-terminated aliphatic SAMs across Au^{TS}/C≡C(CH$_2$)$_n$H//Ga$_2$O$_3$/EGaIn junctions using selected conical tips that were free of visible surface asperities.[3] Solid curves indicate a Gaussian fit.
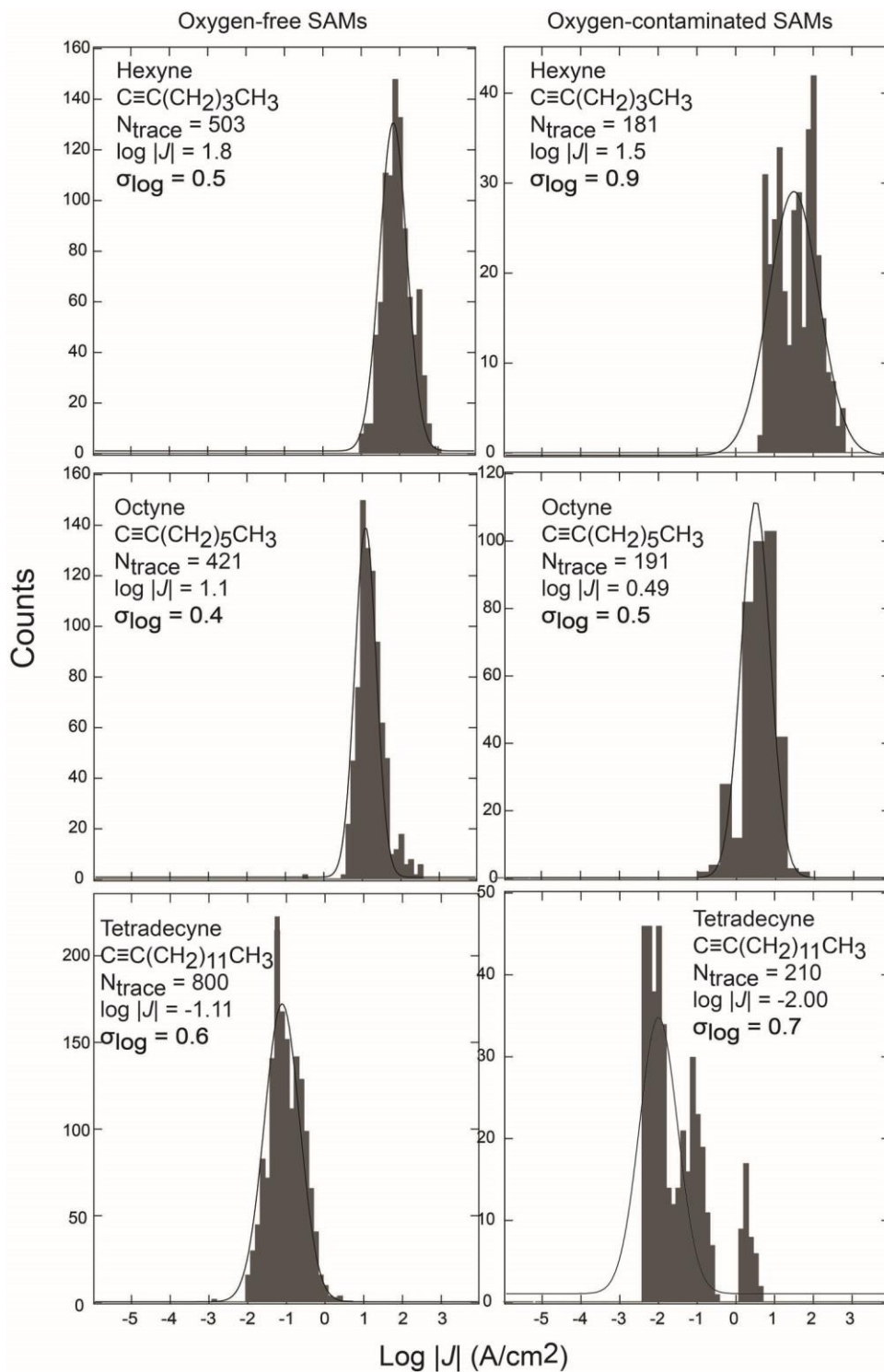
Figure S3. Histograms of log|*J*| at +0.5 V for oxygen-free SAMs (left) and oxygen-containing SAMs (right) across $Au^{TS}C{\equiv}C(CH_2)_nH//Ga_2O_3/EGaIn$ junctions (n = 8, 10, 14) using selected conical tips. Solid curves represent Gassian fits; N is the number of data points.
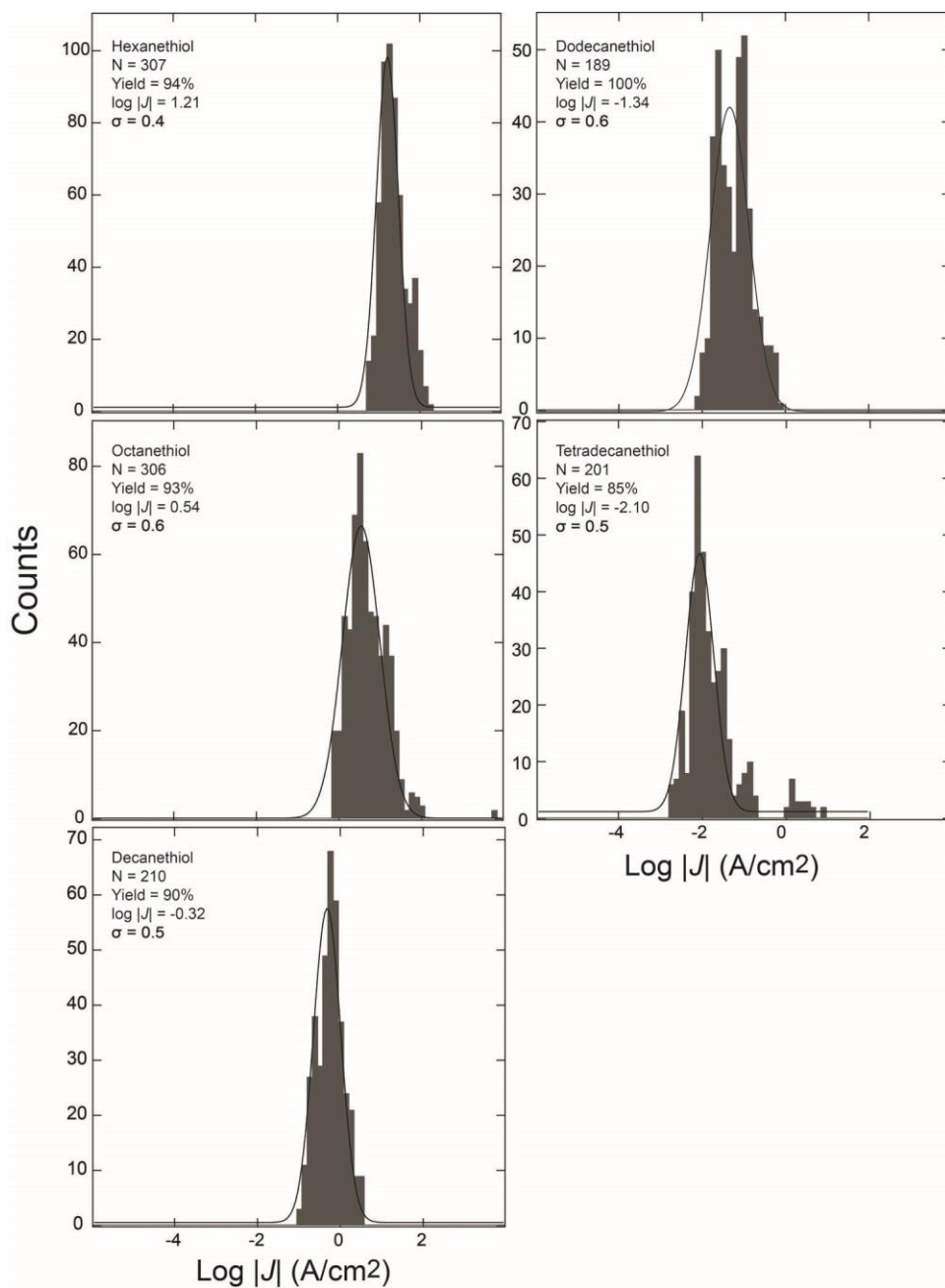
13

Figure S4. Histograms of log|J| at +0.5 V for alkanethiolates using junctions of the structure Au^{TS}S(CH$_2$)$_{2n}$H//Ga$_2$O$_3$/EGaIn junctions (n = 3 − 7) using selected conical tips. Solid curves represent Gassian fits; N is the number of data points.

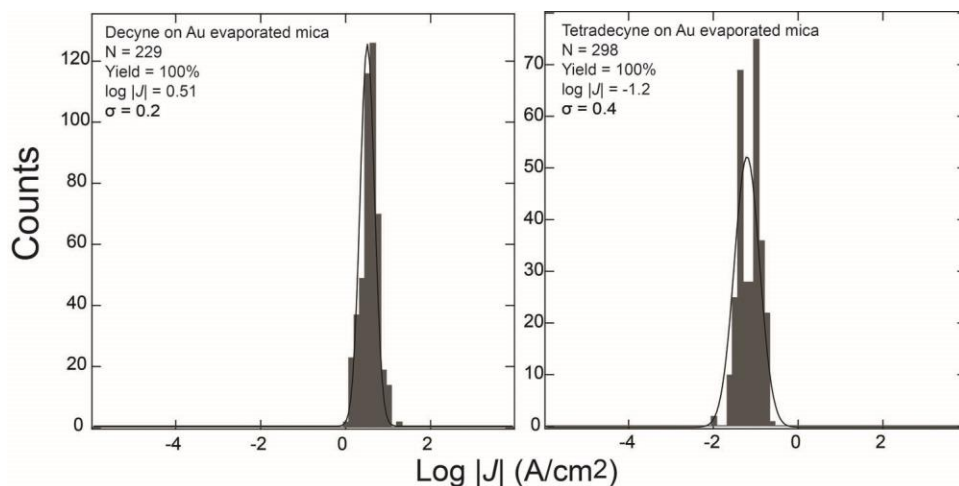**Figure S5**. Histograms of log|J| at +0.5 V for alkynes using junctions of the structure Au^{Mica}C≡C(CH$_2$)$_n$H//Ga$_2$O$_3$/EGaIn junctions (n = 8 and 12) using selected conical tips. Solid curves represent Gassian fits; N is the number of data points. SAMs of decyne and tetradecyne were formed on flame-annealed gold evaporated on mica. The values of log|J| are indistiguishable from those collected on templated-stripped gold (Figure S2).
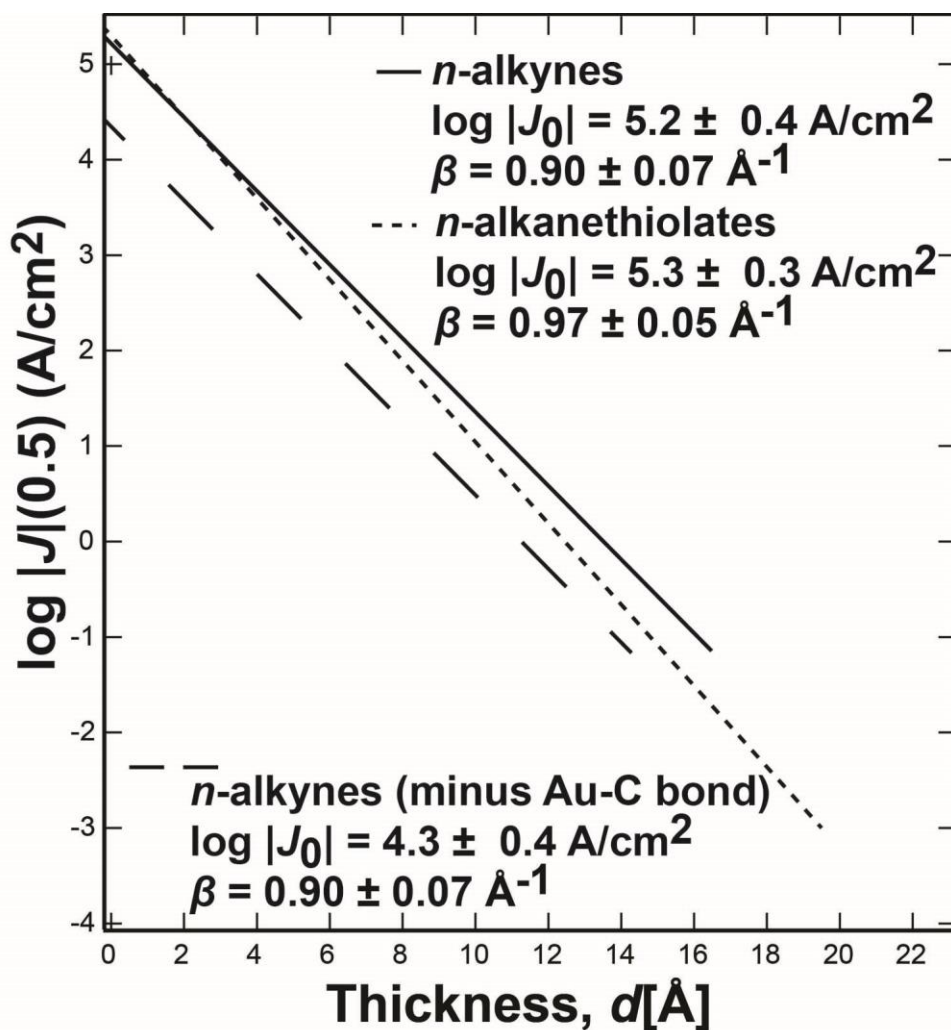
Figure S6. Plot of the Gaussian mean values of log|J| at +0.5 V *versus* thickness for SAMs of *n*-alkynes and *n*-alkanethiolates. The black solid and black small dashed linear-least squares fitting includes the contribution in thickness from the bond to the Au surface. The large dashed linear-least squares fitting excludes the contribution in thickness from the Au-C bond for *n*-alkynes. The thickness values were determined previously using XPS analysis.[10] The differences in J_0 for the n-alkynes (solid black line and grey line) are consistent with the inclusion or exclusion of the Au-C bond from the tunneling barrier. The value of the injection current resulting from the exclusion of the Au-C bond (4.3 A/cm^2) is indistinguishable statistically from that measured from calculating the molecular length for an all-*trans* extended conformation from the first atom of the anchoring group to the final hydrogen atom (4.0 A/cm^2), as represented in Figure 2 of the main text.

REFERENCES

1. Engelkes, V. B.; Beebe, J. M.; Frisbie, C. D. Length-Dependent Transport in Molecular Junctions Based on SAMs of Alkanethiols and Alkanedithiols: Effect of Metal Work Function and Applied Bias on Tunneling Efficiency and Contact Resistance. *J. Am. Chem. Soc.* **2004,** *126*, 14287-14296.

2. Li, X.; He, J.; Hihath, J.; Xu, B.; Lindsay, S. M.; Tao, N. Conductance of Single Alkanedithiols: Conduction Mechanism and Effect of Molecule-Electrode Contacts. *J. Am. Chem. Soc.* **2006,** *128*, 2135-2141.

3. Salomon, A.; Cahen, D.; Lindsay, S.; Tomfohr, J.; Engelkes, V. B.; Frisbie, C. D. Comparison of Electronic Transport Measurements on Organic Molecules. *Adv. Mater.* **2004,** *16*, 1881-1890.

4. Slowinski, K.; Chamberlain, R. V.; Miller, C. J.; Majda, M. Through-bond and chain-to-chain coupling. Two pathways in Electron Tunneling through Liquid Alkanethiol Monolayers on Mercury Electrodes. *J. Am. Chem. Soc.* **1997,** *119*, 11910-11919.

5. Thuo, M. M.; Reus, W. F.; Nijhuis, C. A.; Barber, J. R.; Kim, C.; Schulz, M. D.; Whitesides, G. M. Odd-Even Effects in Charge Transport across Self-Assembled Monolayers. *J. Am. Chem. Soc.* **2011,** *133*, 2962-2975.

6. Thuo, M. M.; Reus, W. F.; Simeone, F. C.; Kim, C.; Schulz, M. D.; Yoon, H. J.; Whitesides, G. M. Replacing -CH$_2$CH$_2$- with -CONH- Does Not Significantly Change Rates of Charge Transport through Ag-^{TS}-SAM//Ga$_2$O$_3$/EGaIn Junctions. *J. Am. Chem. Soc.* **2012,** *134,* 10876-10884.

7. Love, J. C.; Estroff, L. A.; Kriebel, J. K.; Nuzzo, R. G.; Whitesides, G. M. Self-Assembled Monolayers of Thiolates on Metals as a Form of Nanotechnology. *Chem. Rev.* **2005,** *105*, 1103-1169.

8. Liao, K.-C., Yoon, H.J., Bowers, C.M., Simeone, F.C., Whitesides, G. M. Replacing Ag^{TS}SCH$_2$-R with Ag^{TS}O$_2$C-R in EGaIn-based Tunneling Junctions Does Not Significantly Change Rates of Charge Transport. *Angew. Chem., Int. Ed.* **2014,** *53*, 3889-3893.

9. Tao, Y. T. Structural Comparison of Self-Assembled Monolayers of N-Alkanoic Acids on the Surfaces of Silver, Copper, and Aluminum. *J. Am. Chem. Soc.* **1993,** *115*, 4350-4358.

10. Hsu, M. H.; Hu, W. S.; Lin, J. J.; Hsu, Y. J.; Wei, D. H.; Yang, C. W.; Chang, C. S.; Tao, Y. T. H$_2$S-Induced Reorganization of Mixed Monolayer of Carboxylic Derivatives on Silver Surface. *Langmuir* **2004,** *20*, 3641-3647.

11. Tao, Y. T.; Hietpas, G. D.; Allara, D. L. HCl Vapor-Induced Structural Rearrangements of n-Alkanoate Self-Assembled Monolayers on Ambient Silver, Copper, and Aluminum Surfaces. *J. Am. Chem. Soc.* **1996,** *118*, 6724-6735.

12. Weiss, E. A.; Kaufman, G. K.; Kriebel, J. K.; Li, Z.; Schalek, R.; Whitesides, G. M. Si/SiO$_2$-Templated Formation of Ultraflat Metal Surfaces on Glass, Polymer, and Solder Supports: their use as Substrates for Self-assembled Monolayers. *Langmuir* **2007,** *23*, 9686-9694.

13. Yuan, L.; Jiang, L.; Thompson, D.; Nijhuis, C. A. On the Remarkable Role of Surface Topography of the Bottom Electrodes in Blocking Leakage Currents in Molecular Diodes. *J. Am. Chem. Soc.* **2014,** *136*, 6554-6557.

14. Yuan, L.; Jiang, L.; Zhang, B.; Nijhuis, C. A. Dependency of the Tunneling Decay Coefficient in Molecular Tunneling Junctions on the Topography of the Bottom Electrodes. *Angew. Chem., Int. Ed.* **2014,** *53*, 3377-3381.

15. Zaba, T.; Noworolska, A.; Bowers, C. M.; Breiten, B.; Whitesides, G. M.; Cyganik, P. Formation of Highly Ordered Self-Assembled Monolayers of Alkynes on Au(111) Substrate. *J. Am. Chem. Soc.* **2014**, *136*, 11918-11921.

16. Simeone, F. C.; Yoon, H. J.; Thuo, M. M.; Barber, J. R.; Smith, B.; Whitesides, G. M. Defining the Value of Injection Current and Effective Electrical Contact Area for EGaIn-Based Molecular Tunneling Junctions. *J. Am. Chem. Soc.* **2013**, *135*, 18131-18144.

17. Bain, C. D.; Evall, J.; Whitesides, G. M., Formation of Monolayers by the Coadsorption of Thiols on Gold - Variation in the Head Group, Tail Group, and Solvent. *J. Am. Chem. Soc.* **1989,** *111*, 7155-7164.

18. Bain, C. D.; Whitesides, G. M. A Study by Contact-Angle of the Acid-Base Behavior of Monolayers Containing Omega-Mercaptocarboxylic Acids Adsorbed on Gold - an Example of Reactive Spreading. *Langmuir* **1989,** *5*, 1370-1378.

19. Becke, A. D., Density-Functional Thermochemistry .3. The Role of Exact Exchange. *J. Chem. Phys.* **1993,** *98*, 5648-5652.

20. Eichkorn, K.; Treutler, O.; Ohm, H.; Haser, M.; Ahlrichs, R. Auxiliary Basis-Sets to Approximate Coulomb Potentials. *Chem. Phys. Lett.* **1995,** 242, 652-660.

21. Weigend, F. Accurate Coulomb-fitting basis sets for H to Rn. *Phys. Chem. Chem. Phys.* **2006,** *8*, 1057-1065.

22. Andrae, D.; Haussermann, U.; Dolg, M.; Stoll, H.; Preuss, H. Energy-Adjusted Abinitio Pseudopotentials for the 2nd and 3rd Row Transition-Elements. *Theoretica Chimica Acta* **1990,** *77*, 123-141.

23. Cademartiri, L.; Thuo, M. M.; Nijhuis, C. A.; Reus, W. F.; Tricard, S.; Barber, J. R.; Sodhi, R. N. S.; Brodersen, P.; Kim, C.; Chiechi, R. C.; Whitesides, G. M. Electrical Resistance of Ag-^{TS}-S(CH$_2$)(n-1)CH$_3$//Ga$_2$O$_3$/EGaIn Tunneling Junctions. *J. Phys. Chem. C* **2012,** *116*, 10848-10860.

24. Reus, W. F.; Thuo, M. M.; Shapiro, N. D.; Nijhuis, C. A.; Whitesides, G. M. The SAM, Not the Electrodes, Dominates Charge Transport in Metal-Monolayer//Ga$_2$O$_3$/Gallium-Indium Eutectic Junctions. *ACS Nano* **2012,** *6*, 4806-4822.

25. Bowers, C. M., Liao, K.C., Yoon, H.J., Rappoport, D., Baghbanzadeh, M., Simeone, F.C, Whitesides, G.M. Introducing Ionic and/or Hydrogen Bonds into the SAM//Ga$_2$O$_3$ Top-Interface of Ag^{TS}/S(CH$_2$)$_n$T//Ga$_2$O$_3$/EGaIn Junctions. *Nano Lett.* **2014,** *14*, 3521-3526.

26. Simmons, J. G. Generalized Formula for Electric Tunnel Effect between Similar Electrodes Separated by a Thin Insulating Film. *J. Appl. Phys.* **1963,** *34*, 1793-1803.

27. Joachim, C.; Ratner, M. A. Molecular electronics: Some views on transport junctions and beyond. *P. Natl. Acad. Sci. USA* **2005,** *102*, 8801-8808.

28. Yoon, H. J.; Shapiro, N. D.; Park, K. M.; Thuo, M. M.; Soh, S.; Whitesides, G. M. The rate of charge tunneling through self-assembled monolayers is insensitive to many functional group substitutions. *Angew. Chem., Int. Ed.* **2012,** *51*, 4658-4661.

29. Yoon, H. J.; Bowers, C. M.; Baghbanzadeh, M.; Whitesides, G. M. The Rate of Charge Tunneling Is Insensitive to Polar Terminal Groups in Self-Assembled Monolayers in Ag(TS)S(CH$_2$)$_n$M(CH$_2$)$_m$T//Ga$_2$O$_3$/EGaIn Junctions. *J. Am. Chem. Soc.* **2014,** *136*, 16-19.

30. Nerngchamnong, N.; Yuan, L.; Qi, D. C.; Li, J.; Thompson, D.; Nijhuis, C. A. The Role of Van der Waals Forces in the Performance of Molecular Diodes. *Nat. Nanotechnol.* **2013,** *8*, 113-118.

31. Nijhuis, C. A.; Reus, W. F.; Barber, J. R.; Dickey, M. D.; Whitesides, G. M. Charge Transport and Rectification in Arrays of SAM-based Tunneling Junctions. *Nano Lett.* **2010,** *10*, 3611-3619.

32. Nijhuis, C. A.; Reus, W. F.; Siegel, A. C.; Whitesides, G. M. A Molecular Half-Wave Rectifier. *J. Am. Chem. Soc.* **2011,** *133*, 15397-15411.

33. Nijhuis, C. A.; Reus, W. F.; Whitesides, G. M. Mechanism of Rectification in Tunneling Junctions Based on Molecules with Asymmetric Potential Drops. *J. Am. Chem. Soc.* **2010,** *132*, 18386-18401.

34. Yoon, H. J., Liao, Kung-Ching, Lockett, Matthew R., Kwok, Sen Wai, Baghbanzadeh, Mostafa, Whitesides, George M., Rectification in Tunneling Junctions: A Rectifier Using 2,2'-Bipyridyl-terminated n-Alkanethiolates. **Submitted**.

35. Fracasso, D.; Valkenier, H.; Hummelen, J. C.; Solomon, G. C.; Chiechi, R. C. Evidence for Quantum Interference in SAMs of Arylethynylene Thiolates in Tunneling Junctions with Eutectic Ga-In (EGaIn) Top-Contacts. *J. Am. Chem. Soc.* **2011,** *133*, 9556-9563.